ACS APPLIED POLYMER MATERIALS

Article

High Performance Transparent Laminates based on Highly Oriented Polyethylene Films

Yunyin Lin, Jun Cao, Mei-Fang Zhu, Emiliano Bilotti, Han Zhang, Cees W. M. Bastiaansen, and Ton Peijs

ACS Appl. Polym. Mater., **Just Accepted Manuscript** • DOI: 10.1021/acsapm.0c00404 • Publication Date (Web): 26 May 2020

High Performance Transparent Laminates based on Highly Oriented Polyethylene Films

Yunyin Lin [a], Jun Cao [a], Meifang Zhu [c], Emiliano Bilotti [a,b], Han Zhang [a,b], Cees W. M. Bastiaansen *[,a,d], Ton Peijs *[,e]

[a] School of Engineering and Materials Science, Queen Mary University of London, Mile End Road, London E1 4NS, U.K.

[b] Nanoforce Technology Ltd., Mile End Road, London E1 4NS, U.K.

[c] State Key Laboratory for Modification of Chemical Fibers and Polymer Materials & College of Materials Science and Engineering, Donghua University, Shanghai 201620, China

[d] Laboratory of Functional Organic Materials and Devices, Eindhoven University of Technology, P.O. Box 513, Eindhoven 5600 MB, The Netherlands

[e] Materials Engineering Centre, WMG, University of Warwick, Coventry CV4 7AL, U.K.

* **Corresponding Authors.** E-mail address: t.peijs@warwick.ac.uk (T. Peijs) and c.w.m.bastiaansen@tue.nl (C.W.M. Bastiaansen).

Abstract

Advanced composite materials reinforced with high performance fibers like carbon, glass, aramid or ultra-high molecular weight polyethylene are widely used as lightweight materials in the fields of automotive, aerospace, sports and protection. However, nearly always these composites are opaque and/or they absorb light, which greatly limits their application in areas where high optical

transparency is desired such as impact resistant windows and visors. In this work, composite laminates that combine high optical clarity with high mechanical properties are reported for the first time using highly oriented high-density polyethylene (HDPE) films as the reinforcing phase. A high optical transparency with a far field light transmittance of around 85 % was achieved for 4-layer HDPE-reinforced laminates sandwiched between glass or polycarbonate (PC) sheets with either unidirectional (UD) or bidirectional (BD) orientations. In combination with outer layers of glass or PC, the fabricated transparent composite laminates show a high tensile strength and also a high penetration energy absorption, outperforming existing transparent materials like glass, laminated glass or PC. These transparent composites combine both high mechanical performance and high optical clarity, providing great potential for future applications in structural glazing, automotive glazing, safety shields, visors and displays for portable electronics.

Graphical Abstract

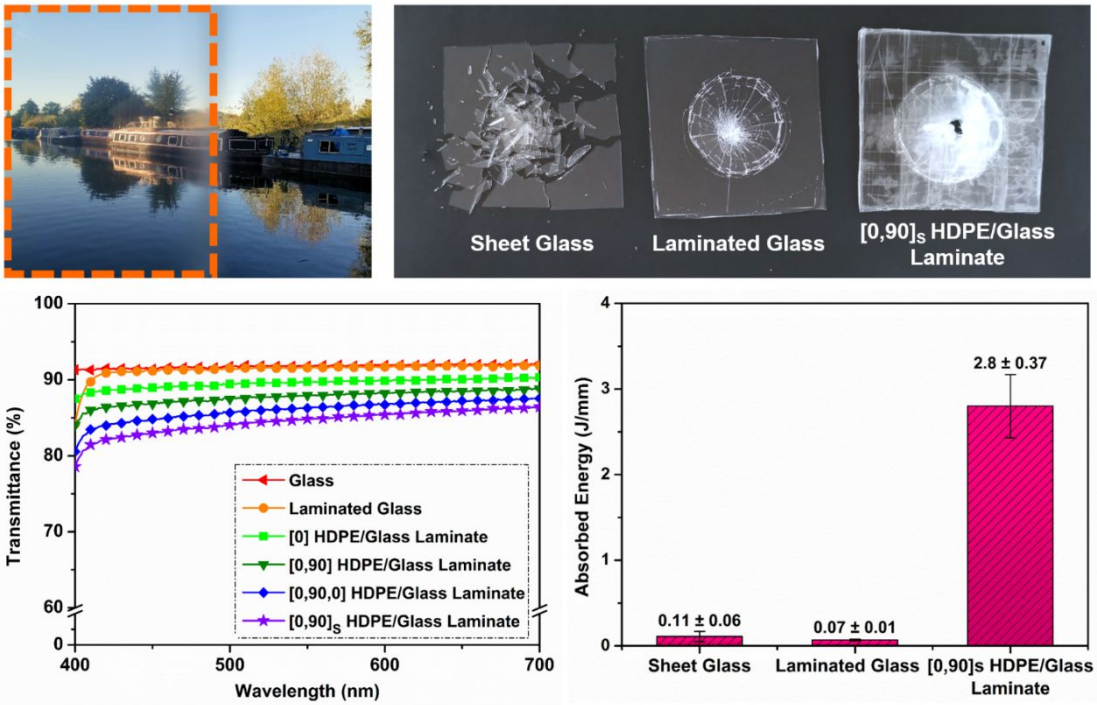

Keywords

Laminated glass, transparent composites, polyethylene, mechanical properties, impact resistance.

1. Introduction

Composite laminates reinforced with high performance fibers such as carbon[1-3], glass[4], polyethylene (PE)[5-6] and aramids[7], are increasingly used in aerospace, automotive, sports, and other fields like renewable energy owing to their high specific modulus and strength. Unlike high modulus carbon fibers with relatively low strains at break, high performance ultra-high molecular weight polyethylene (UHMWPE) fibers like Dyneema® or Spectra® and aramid fibers like Kevlar® and Twaron® possess not only high specific stiffness and tensile strength but also relatively high levels of toughness with the ability to absorb large amounts of energy upon fracture, leading to various applications where impact resistance is of great importance such as bullet-proof vests, armor, helmets and anti-ballistic composites[6, 8-10].

However, high performance composites are typically non-transparent due to severe light scattering effects caused by the large surface area of the reinforcing fibers and differences in refractive indices between fibers and matrix. Besides, fibers like aramid and carbon absorb light, which renders them impractical for producing transparent composite laminates. Some efforts were made in fabricating transparent composites by matching the refractive indices of the polymer matrix and the reinforcing phase, including S-glass fibers[11-12], glass ribbons[13-14], nylon fibers[15-16], cellulose nanofibers[17-19] and drawn polypropylene (PP) filaments[20]. However, most of these laminated composites only achieved limited optical transparency especially in the far field as required in windows and visors.

Common transparent materials such as inorganic glass or amorphous polymers are extensively used in applications requiring a high clarity, whilst their mechanical performance is rather limited. For instance, glass combines a high clarity with scratch resistance but is typically brittle and has a low strength (< 50 MPa). This results in safety issues when using glass in structural applications such as car windshields and glazing elements as fracture typically involves shattering into multiple fragments, potentially causing injuries to occupants[21]. Some efforts have been made to enhance the mechanical characteristics of glass by lamination with transparent polymeric interlayers such as polyvinyl butyral (PVB), ethylene-vinyl acetate (EVA) or thermoplastic polyurethane (TPU), with the main purpose to preserve the integrity of glazing and to prevent it from scattering into multiple fragments. However, strength and impact resistance of laminated glass is still rather low compared to those of some high performance composites[22-25]. Typical polymeric transparent materials like polycarbonate (PC) and poly(methyl methacrylate) (PMMA) generally possess a low modulus (2−3 GPa) compared to glass and a low strength (~ 60 MPa) compared to high performance composite materials[26]. Also, the poor scratch resistance of these polymeric materials makes such products less durable in long-term usage.

Very recently, ultra-drawn high-density polyethylene (HDPE) films possessing a high strength and high stiffness in combination with high optical clarity were successfully produced by cast film extrusion and solid-state drawing[27-29]. These transparent high strength HDPE films open new avenues towards the development of high performance transparent laminated composites.

In this work, highly oriented transparent HDPE films with unidirectional (UD) or bidirectional (BD) orientations were used as the reinforcing phase in composite laminates with either glass or PC as outer layers. The study also involved the selection of an appropriate interlayer material that ensures high optical clarity together with good adhesive bonding. Apart from a high far field

optical transparency (~ 85 %), all HDPE-reinforced laminates demonstrated a high mechanical performance. Significantly improved energy absorption capabilities were obtained, with a more than 25 times higher penetration energy for BD [0,90]s HDPE laminates with glass as outer layers compared to pure sheet glass, and a nearly two times higher work-to-break for UD $[0]_4$ HDPE laminates with PC as outer layers compared to pure PC. Potential applications of these high performance lightweight transparent laminated composites are proposed in the fields of aerospace, automotive, building and construction, and opto-electronics.

2. Experimental

2.1. Materials

The high-density polyethylene (HDPE) used in this work was Borealis VS4580 (Borealis AG, Austria). It was received in pellet form with a density of 0.958 g/cm^3, a melting temperature (T_m) of 134 °C and a melt flow index (MFI) of 0.6 g/10 min at 190 °C/2.16 kg and 21 g/10 min at 190 °C/21.6 kg. As an outer layer material, D 263® T eco, a borosilicate glass with a thickness of 210 μm was used which was supplied by Schott AG (USA). Polycarbonate (PC) 801E films with a thickness of 25 μm were provided by Sichuan Longhua Film Co., Ltd. (China) and RS Pro Clear PC sheets with a thickness of 1 mm were purchased from RS Components (UK). As an adhesive interlayer material, thermoplastic polyurethane (TPU) ST-6050 sheets were used which were provided by Schweitzer-Mauduit International, Inc. (USA). Ethylene vinyl acetate (EVA) EVAevguard® Clear sheets and polyvinyl butyral (PVB) Everlam™ Clear sheets were purchased from Qdel laminating solutions (Netherlands). 2-Butanone (99.5 %, GC) and Ethylene glycol (99.8 %) were purchased from Sigma-Aldrich (USA).

2.2. Preparation of Specimens

Highly oriented solid-state drawn transparent HDPE films were manufactured using continuous cast film extrusion and solid-state drawing process using a Collin E20T (Germany) single screw extruder and a Collin MDO-A & MDO-B (Germany) uniaxial stretching line, as described in our previous publication[28]. These oriented films possess a pre-orientation ratio (so-called draw down) of ~ 4, a solid-state draw ratio of ~ 15 and a final average thickness of around 30 μm. The mechanical properties of these uniaxial films were reported previously: the films have a Young's modulus of approximately 12 GPa, a tensile strength of 440 MPa and a strain-at-break of 25 % in the drawing direction[28]. The transverse properties of these highly anisotropic PE films are significantly lower: a Young's modulus of ~ 2 GPa and tensile strength of ~ 15 MPa[30]. Mechanical properties of the laminate constituent materials are listed in Supporting Information ***Table S1***.

Clearly, orientation of the uniaxial HDPE films within the laminate has a great influence on the mechanical properties of the composites. Unidirectional (UD) laminates will be very stiff and strong along the drawing or 0° direction of the film, whereas they will be weak in the transverse 90 direction. Such laminates will deliver ultimate mechanical performance, albeit only when loaded uniaxially in tension. Bidirectional (BD) composites with a 0°/90° lay-up are more applicable for most multi-axially loaded engineering applications[31-32]. Here, we evaluated both UD and BD laminate configurations but these uniaxially oriented HDPE films allow for a multitude of laminate designs, including quasi-isotropic lay-ups like 0°/60°/-60° or 0°/45°/-45°/90°.

In order to cover a wide spectrum of properties and applications, UD and BD laminate lay-ups were manufactured and evaluated in this study: (i) UD laminates with four layers of unidirectionally stacked HDPE films with a $[0]_4$ stacking sequence (***Figure 1(a)***), and (ii) BD

laminates with four layers of cross-plied HDPE films with a $[0,90]_S$ stacking sequence sandwiched between either glass (***Figure 1(b)***) or PC.

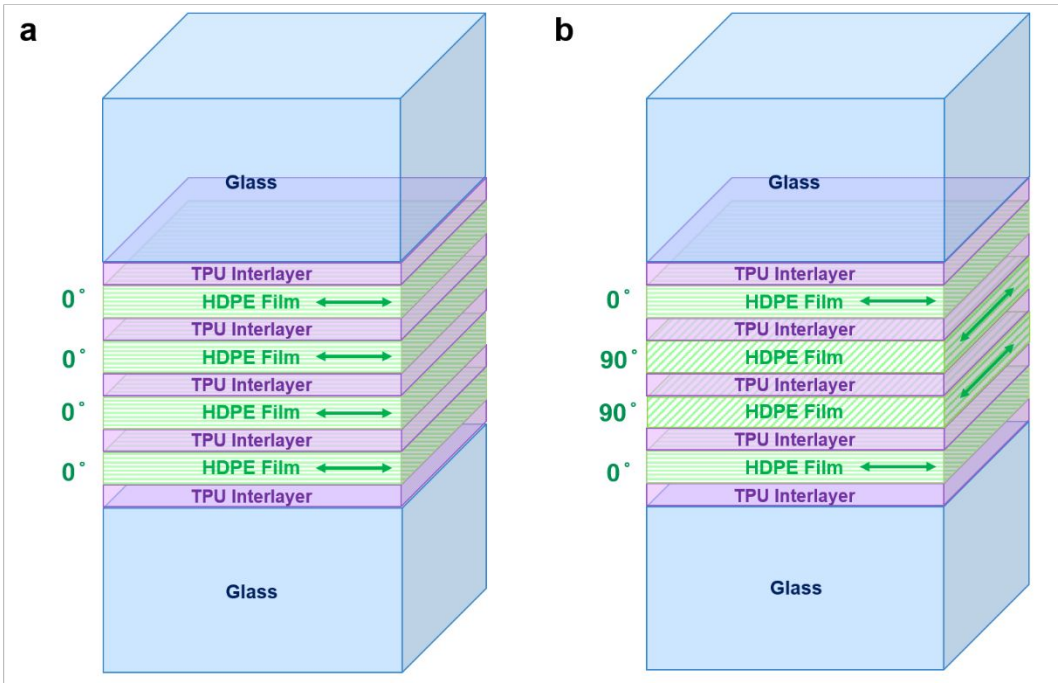

Figure 1. Schematic diagram of different HDPE laminate designs with sheet glass (210 µm) as outer layers: (a) unidirectional (UD) and (b) bidirectional (BD) stacking of oriented HDPE films with TPU coatings as interlayers. PC is also be used as outer layers but has a much lower thickness (25 µm) than glass, similar to HDPE (30 µm). Relative thickness of the different layers drawn to scale.

The selection of TPU as interlayers in the laminates will be discussed in detail with regards to optical, thermal and adhesive properties in Section 3.1. In order to obtain thin TPU interlayers for bonding glass or PC outer layers to HDPE film or between HDPE films, TPU sheets (380 µm) were cut into pieces and dissolved at 5 wt.% in 2-butanone at 80 °C for 2 h until the solution became homogeneous and clear. Next, 1 mL of this 5 wt.% TPU/2-butanone solution was dip-

coated at room temperature (RT) onto both sides of the oriented HDPE films with a surface area of about 25 cm^2. After evaporation of the solvent in a fume hood at 60 °C overnight, HDPE films with a thin (~ 10 μm) TPU coating on both sides were obtained. Subsequently, these TPU-coated HDPE films were stacked together with sheet glass (210 μm) or PC sheets (25 μm) as outer layers in a lay-up sequence as indicated in ***Figure 1***. The interlayer thickness between HDPE and glass or PC was around 10 μm and doubled to around 20 μm between the dip-coated HDPE films. The corresponding laminates were compression molded using a Rondol (UK) hot press at 100 °C, 20 bar for 10 min, i.e. well below the melting temperature of the HDPE (134 °C) to prevent chain relaxation and loss of mechanical properties of the oriented HDPE films.

2.3. Characterization

The contact angles between a liquid droplet and layer materials were measured using a KRÜSS DSA100 (Germany) drop shape analyzer. A 5 μL sessile droplet of distilled water or ethylene glycol was dropped onto the surface of the solid layer and the contact angle was measured using Drop Shape Analysis software. The surface free energy (or surface tension) was calculated to obtain information on the wettability between layers and interlayers using the Owens-Wendt-Rabel-Kaelble (OWRK) model[33], which is suitable for most of materials, including polymers like PC and TPU. In this theory, the surface free energy of a solid material is assumed to be composed of two components: (1) a dispersive part originating from van der Waals and other apolar interactions; (2) a polar part originating from hydrogen bonding, dipole-dipole, dipole-induced dipole and other secondary interactions. This model is mainly based on the Young's equation (eq. (1)) and Good's equation (eq. (2))[34-35]:

$$\gamma_s = \gamma_{sl} + \gamma_l \cos\theta \tag{1}$$

$$\gamma_{sl} = \gamma_s + \gamma_l - 2\sqrt{\gamma_s^d \gamma_l^d} - 2\sqrt{\gamma_s^p \gamma_l^p} \tag{2}$$

where γ_{sl} is the interfacial free energy between a solid and a liquid; γ_s and γ_l are the surface free energy of the solid or the liquid; θ is the contact angle between the solid and the liquid; γ_s^d, γ_l^d, γ_s^p, γ_l^p are the dispersive (*d*) or polar (*p*) component of the surface free energy of the solid (*s*) and the liquid (*l*), respectively.

Combining eq. (1) and (2) leads to the following equation:

$$\frac{\gamma_l(\cos\theta + 1)}{2\sqrt{\gamma_l^d}} = \sqrt{\gamma_s^p}\frac{\sqrt{\gamma_l^p}}{\sqrt{\gamma_l^d}} + \sqrt{\gamma_s^d} \tag{3}$$

Eq. (3) is equivalent to a linear equation $y = ax + b$, where:

$$y = \frac{\gamma_l(\cos\theta + 1)}{2\sqrt{\gamma_l^d}}; \quad a = \sqrt{\gamma_s^p}; \quad x = \frac{\sqrt{\gamma_l^p}}{\sqrt{\gamma_l^d}}; \quad b = \sqrt{\gamma_s^d} \tag{4}$$

Thus, the overall, dispersive part and polar part of the surface free energy of a solid material can be obtained by fitting a linear equation to the contact angle data for at least two types of liquid on a solid. The interfacial free energy between two solid or semi-solid materials, like two viscoelastic polymers, can also be calculated by eq. (2) from the solid surface free energy of these two materials[36].

Transmission spectra of the laminates were measured using a PerkinElmer Lambda 950 (USA) UV-vis spectrometer in the wavelength range of 300−700 nm at an interval of 1 nm. A sample-to-detector distance of 40 cm was used to obtain transmittance values in the far field rather than in the near field, which is of greater practical importance for applications like windows or visors[27]. Transmission spectra were measured in triplicate for each laminate type. Optical micrographs were

recorded on an Olympus BX60 (USA) microscope in transmission-mode between crossed polarizers.

T-peel tests, tensile tests and quasi-static penetration tests were all carried out in an Instron 5566 (UK) universal tensile tester at RT. T-peel tests were carried out to evaluate interlaminar bonding at a constant crosshead speed of 254 mm/min in accordance with ASTM 1876-08[37]. For T-peel test specimens, the interlayer material was sandwiched between two oriented HDPE films as shown in ***Figure 2(a)*** in Section 3.1 and then compression molded using a Collin P300E (Germany) hot press at a pressure of 20 bar. Different temperatures were used for each type of interlayer (100 °C for TPU, 90 °C for EVA and 120 °C for PVB) and these temperatures were selected based on their thermal properties (see Section 3.1). T-peel specimens were used with a width of 25 mm, a bond length of 241 mm and an unbonded length of 76 mm (for clamping inside the pneumatic side action grips). The normalized peel force (N/mm) was defined as the force per unit width of the specimen required to produce progressive separation of the two bonded films. The average normalized peel force for crack propagation was calculated over the extension range of 150−400 mm by integrating the area below the normalized peel force-extension curves and dividing this by the extension range (250 mm). At least five specimens were measured to ensure reproducibility.

For tensile tests, rectangular-shaped laminates with a dimension of 100 mm × 10 mm were prepared by compression molding. In order to avoid stress concentration at the clamps, tapered end-taps of PC sheets with a thickness of 1 mm and a tab length of 25 mm were bonded to the laminates using TPU as an adhesive. Samples were clamped in manual wedge action grips and tests were carried out at a constant crosshead speed of 2 mm/min according to ASTM D3039-17[38]. The Young's modulus was calculated from the tangent of the engineering stress-strain curve at a

strain below 0.5 %. The average Young's moduli and tensile strengths in combination with their standard deviation were calculated from at least five repeats.

For the quasi-static penetration tests, square-shaped laminates with a dimension of 50 mm × 50 mm were clamped between two steel plates, which had an internal circular opening with a diameter of 30 mm. A hemispherical dart with a diameter of 10 mm was used and a constant dart speed of 1.25 mm/min was employed during these quasi-static dart penetration tests in accordance with ASTM D6264-17[39]. Only BD laminates were tested considering the multi-directional loading nature of this test. Energy absorption required for full penetration was obtained by integrating the area under the force-displacement curve during the penetration process. The contact force, absorbed energy and peak force were all normalized by specimen thickness.

3. Results and discussion

3.1 Interlayer selection

To ensure a high optical transparency together with a high mechanical performance, interlayer materials with a refractive index close to the other materials and good adhesive bonding to the reinforcing HDPE phase are required. Therefore, a systematic study was performed to evaluate some common interlayer materials prior to transparent composite fabrication.

For laminated glass with high clarity, commonly used polymeric interlayers include PVB, EVA and TPU. All these three interlayer materials are employed here to assess their performance in current HDPE transparent composites. ***Table 1*** shows that specimens sandwiched between glass have a slightly higher transmittance than those sandwiched between PC at a wavelength of 550 nm, presumably due to the smaller refractive index mismatch between TPU and glass. The use of

TPU results in a slightly higher transmission than EVA and PVB for both types of laminates, again as a result of the smaller refractive index mismatch between TPU and the glass or PC. In comparison to EVA and PVB, the refractive index of TPU (n = 1.50) is closer to glass (n = 1.50−1.52)[21], PC (n = 1.58−1.60)[40] and birefringent HDPE films (with an average refractive index of 1.54)[41]. As a consequence, the extent of light reflection at each interface decreases and therefore more light is transmitted through the laminates using TPU as interlayers. A more detailed analysis of the optical properties of the different interlayers is presented in Supporting Information (***Figure S1***).

Table 1. Comparison among TPU, EVA and PVB interlayers with respect to compression molding temperature, refractive index, transmittance at a wavelength of 550 nm when sandwiched between glass or PC tested at a 40 cm sample-to-detector distance and average peel force from T-peel tests.

Material	Lamination Temperature (C)	Refractive Index	Transmittance between Glass (%)	Transmittance between PC (%)	Average Normalized Peel Force (N/mm)
TPU	100	1.50	91.6 ± 0.2	89.9 ± 0.3	0.150 ± 0.061
EVA	90	1.48−1.49	91.4 ± 0.1	89.4 ± 0.2	0.080 ± 0.013
PVB	120	1.48	91.0 ± 0.1	88.8 ± 0.2	0.043 ± 0.008

DSC curves revealing the thermal properties of each material including the three interlayer materials are shown in Supporting Information ***Figure S2***. EVA shows two significant melting endotherm peaks in the temperature range of 25−87 °C, corresponding to melting of less perfect crystals at a low temperature and more perfect organized crystals at higher temperature[42]. Hence, 90 °C was chosen for lamination using EVA interlayers. TPU has a melting endotherm peak

between 60−95 °C, and therefore for this interlayer system a lamination temperature of 100 °C was used. PVB exhibits a glass transition temperature (T_g) at ~ 16 °C[43]. Through actual compression molding trials, it was found that PVB did not melt or flow until 120 °C. Since the lamination temperature cannot be too close to the melting point of HDPE (T_m ~ 134 °C), as this will result in loss of molecular orientation due to chain relaxation or even melting, PVB was compression molded at a maximum temperature of 120 °C. In terms of outer layers, PC and sheet glass have both thermal stabilities well above the molding temperature range of 90−120 °C.

Interfacial bonding was investigated by T-peel tests, which examined the resistance to Mode-I peeling failure between different layers for all three interlayer materials. In ***Table 1*** and ***Figure 2(b)***, it is shown that the average peel force required to separate two oriented HDPE films adhesively bonded together by a TPU interlayer is nearly twice and 3.5 times than that of EVA or PVB, respectively. In all cases, after T-peel testing the interlayers only adhered to one of the two films, indicating interfacial adhesive failure between interlayer and HDPE film for all three interlayer materials. However, obvious splitting of the oriented HDPE films is observed in the case of TPU as shown in ***Figure 2(c)***, which suggests good load transfer between TPU and HDPE and which is in clear contrast to the smooth fracture surface with PVB or EVA, where peeling is dominated by adhesive interface failure. Tensile properties of the three interlayer materials are also shown in Supporting Information (***Figure S3*** and ***Table S2***).

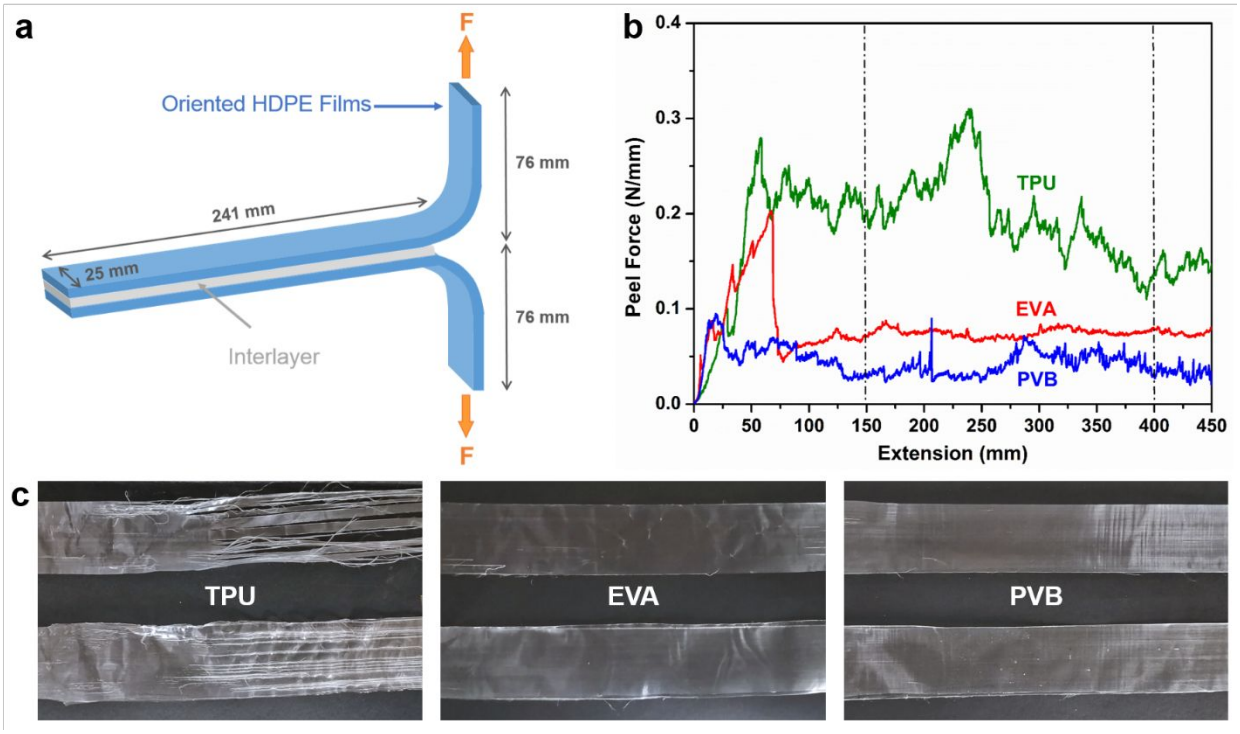

Figure 2. (a) Schematic diagram of T-peel test sample, (b) peel force versus extension curves from T-peel tests of different interlayers between two oriented HDPE films after lamination by hot pressing and (c) appearance of T-peel specimens with different interlayers after testing, showing HDPE fibrillation in the case of TPU interlayer indicative of strong adhesive bonding.

Because of the brittleness of the thin sheet glass, the adhesion properties between glass and the adhesives interlayer materials are difficult to determine by T-peel tests. Instead, contact angles of outer layer materials (glass and PC), reinforcing phase (oriented HDPE) and interlayer materials (TPU, EVA and PVB) and corresponding solid surface free energies were measured and calculated (see Supporting Information ***Table S3***). Improved wetting is expected by a lower contact angle and higher solid surface free energy. On the basis of the solid surface free energies, the corresponding interfacial free energies between different adjacent layers used in the laminates were calculated using eq. (2) and are listed in ***Table 2***. The interfacial free energy between glass

and HDPE is 68.8 ± 1.04 mN/m, which is the highest among all values in ***Table 2***, indicating the weakest interfacial interaction between them among all interfaces. In fact, glass and the HDPE film will not stick to each other at all unless the HDPE is melted, which is why an adhesive interlayer is needed to bond them together in a laminate. After incorporating polymeric interlayers between the glass and HDPE, the interfacial free energies at these new interfaces are significantly reduced. PVB possesses the lowest interfacial free energy when in contact with glass, which is why PVB is widely used in commercial laminated glass, while TPU had again a lower interfacial free energy compared to EVA. However, TPU and EVA have a lower interfacial free energy than PVB when in contact with PC or HDPE. Since a lower interfacial free energy is desirable for better wetting and adhesive bonding[33], it can be concluded that TPU provides the best overall balance in wetting and interfacial bonding with glass, PC and HDPE in comparison to EVA and PVB. It should be noted that surface modifications like corona or plasma treatments could be used to modify the surface of HDPE films by introducing some functional groups and improved adhesive bonding[30].

Table 2. Interfacial free energy (mN/m) calculated between adjacent layers in laminates.

Material	Glass	PC	HDPE
TPU	31.8 ± 0.16	1.10 ± 0.01	7.94 ± 0.35
EVA	45.8 ± 0.26	2.06 ± 0.03	5.40 ± 0.56
PVB	12.0 ± 0.05	8.61 ± 0.12	23.2 ± 0.52

From the above analysis of optical properties, average peel force and interfacial free energy, TPU was selected as the interlayer of choice for the current transparent HDPE laminates.

3.2 Optical properties of HDPE laminates with glass as outer layers

In most studies claiming optical transparency, the "transparent" specimen is positioned close to or directly on top of a background image or at a very short distance from an object[44-45], which is usually considered as optical transparency in the near field. However, actual transmittance generally refers to the ability of an observer to a non-distorted view through a relatively distant sample and object which is far away (ASTM D1746-15)[46], in a similar way as one observes a distant scenery through a window. Therefore, here the optical appearance of the UD and BD HDPE composite laminates with glass as outer layers is examined when the laminates are positioned in front of a distant scenery as shown in ***Figure 3(a)-(b)***, representing the appearance of the laminates in the so-called far field. It is shown that both UD and BD laminates have a highly transparent appearance and the distant scenery can be clearly seen with only minor differences between the laminate covered section (left) and the uncovered section (right). Clearly, both $[0]_4$ and $[0,90]_S$ TPU coated HDPE laminates possess a high optical transparency when sandwiched between glass, even at a distance from the object.

To study the effect of the number of reinforcing HDPE layers on the optical transmittance of the resulting composite laminates, laminates with different numbers of TPU coated HDPE films were analyzed by UV-vis transmittance spectra using a sample-to-detector distance of 40 cm to mimic the far field. The transmittance of HDPE laminates with glass as outer layers in the visible light wavelength regime is presented in ***Figure 3(c)-(d)*** and Supporting Information ***Table S4***. It is shown that UD and BD HDPE/glass laminates with an identical number of HDPE layers have similar transmittance values. In addition, it is found that introducing an additional layer of TPU coated HDPE to the laminates will lead to a transmittance drop of around 1−2 % in the visible light

range. The drop in transparency at 550 nm as measured with the UV-vis might seem surprising especially in view of the photographs presented in ***Figure 3(a)-(b)***.

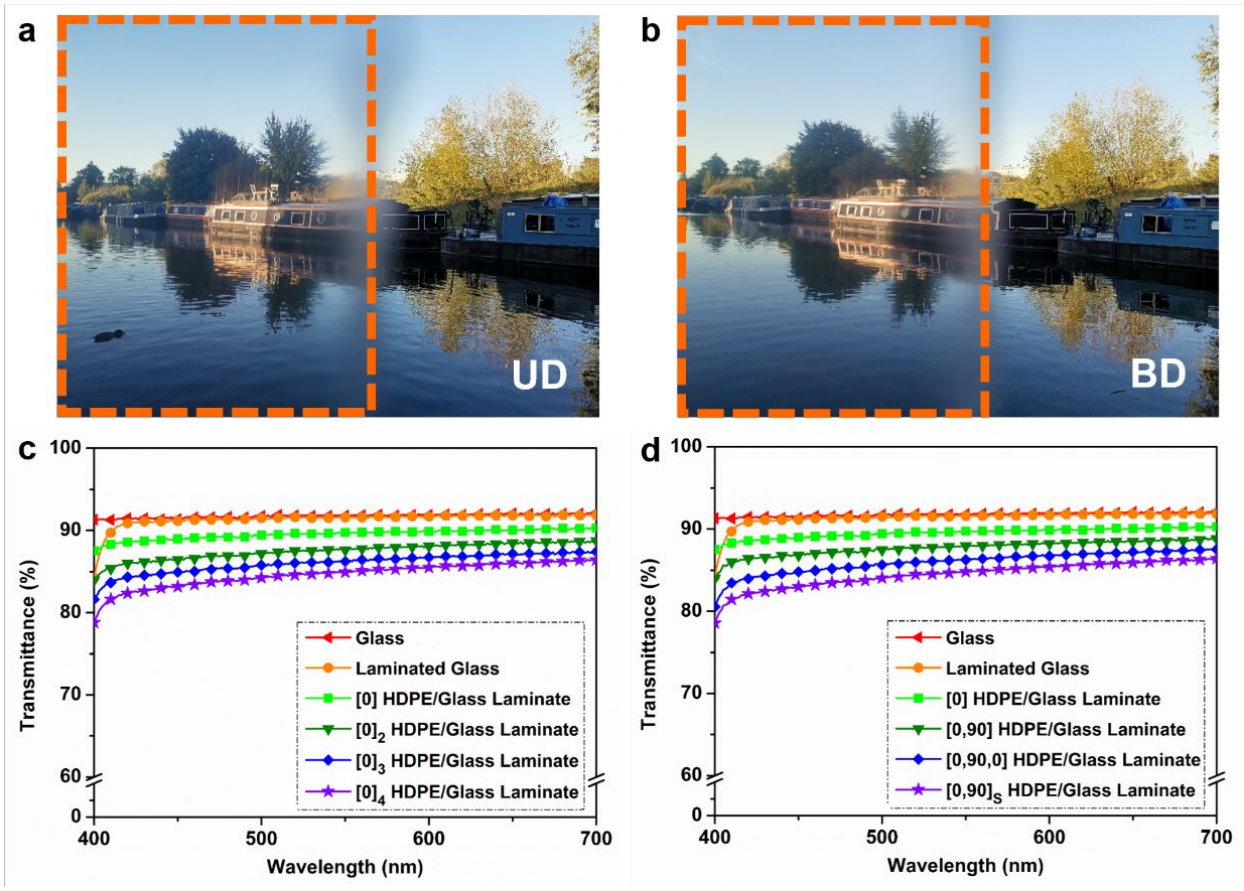

Figure 3. Optical appearance of (a) $[0]_4$ and (b) $[0,90]_S$ HDPE laminates with glass as outer layers when positioned in front of a distant scenery, showing a clear appearance for both UD and BD HDPE/glass laminates in the far field. For clarity, the dashed box sections in (a) and (b) mark the position of the laminates in front of the image. Transmittance spectra of (c) UD and (d) BD HDPE/glass laminates with different numbers (1, 2, 3, 4) of oriented HDPE layers measured at a sample-to-detector distance of 40 cm in the visible wavelength range, indicating a reduction in transmittance in the far field of around 1−2 % with every additional layer of TPU coated HDPE.

Laminates with a single layer of oriented HDPE possess a transmittance value of ~ 90 % at 550 nm, while for four layers of HDPE, the transmittance values of UD and BD HDPE/glass laminates are around 85 %. It is believed that this transmittance loss with increasing numbers of HDPE layers is mainly the result of the increasing number of interfaces between HDPE films and TPU interlayers. At these interfaces, increased light reflection is to be expected due to the, albeit small, refractive index difference between the birefringent and solid-state stretched HDPE[47-48] and the optically isotropic TPU. In other words, anisotropic adhesive layers need to be identified to generate refractive index matching in three dimensions if this drop in transmittance is to be avoided or reduced. Additional light scattering can also contribute to the transmittance drop as a result of increased defects, impurities and dust in or between the layers. At the moment, however, we believe that this is a minor effect which can be resolved by working in a clean environment with more or less standard precautions for dust control, etc.

3.3 Penetration resistance of HDPE laminates with glass as outer layers

The penetration resistance of HDPE laminates with glass as outer layers was studied by quasi-static dart penetration tests. Since failure of UD laminates during such a test will merely lead to transverse splitting of the highly anisotropic films and brittle fracture with limited energy absorption[49], only BD laminates were considered to evaluate the penetration resistance of these transparent HDPE/glass laminates.

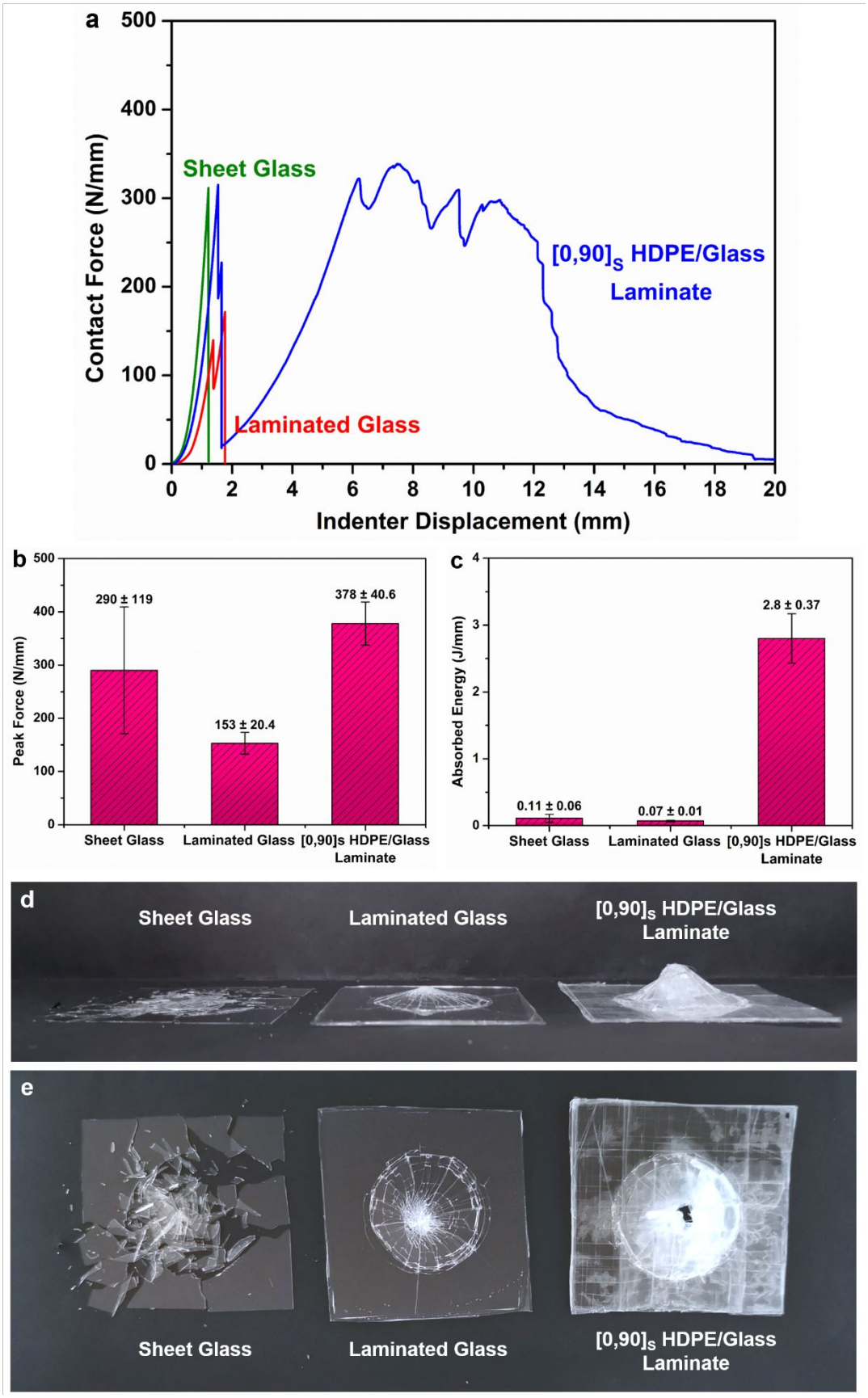
a
Contact Force (N/mm)
Indenter Displacement (mm)
Sheet Glass
Laminated Glass
[0,90]S HDPE/Glass Laminate
b
Peak Force (N/mm)
290 ± 119
153 ± 20.4
378 ± 40.6
Sheet Glass
Laminated Glass
[0,90]s HDPE/Glass Laminate
c
Absorbed Energy (J/mm)
0.11 ± 0.06
0.07 ± 0.01
2.8 ± 0.37
Sheet Glass
Laminated Glass
[0,90]s HDPE/Glass Laminate
d
Sheet Glass
Laminated Glass
[0,90]S HDPE/Glass Laminate
e
Sheet Glass
Laminated Glass
[0,90]S HDPE/Glass Laminate

Figure 4. (a) Contact force versus indenter displacement, (b) peak force and (c) absorbed energy of sheet glass, laminated glass and $[0,90]_S$ HDPE laminates with glass as outer layers. It shows that the BD HDPE/glass laminate can absorb more than 25 times the energy of sheet glass or laminated glass. (d) Edge-side view of tested laminates with large out-of-plane deformation in the case of BD HDPE laminate sandwiched between glass and (e) bottom-side view of penetration damage of sheet glass, laminated glass and BD HDPE/glass laminate, indicating significant energy absorption by delamination and improved structural integrity after full penetration for the latter. Contact force, absorbed energy and peak force are all normalized by specimen thickness to enable a fair comparison.

Figure 4(a) shows the normalized contact force as a function of indenter displacement for sheet glass, laminated glass with TPU interlayers, and BD $[0,90]_S$ HDPE laminate with glass as outer layers. For both sheet glass and laminated glass specimens, the contact force dropped to zero at a low displacement (< 2 mm) due to the inherent brittle nature of glass. On the other hand, although a clear drop was also observed at a similar low displacement for the BD HDPE/glass laminate as a result of fracture of the glass outer layers, these laminates showed pseudo-ductile behavior with the contact force increasing again with further displacement, until final fracture of the laminate at around 20 mm displacement.

The normalized peak force for the BD HDPE/glass laminate reached 378 N/mm, higher than for both sheet glass (290 N/mm) and laminated glass with a TPU interlayer (153 N/mm) as shown in ***Figure 4(b)***. This can be attributed to the reinforcing HDPE phase, providing increased strength together with good load transfer between the layers due to the adhesive TPU interlayers. Interestingly, because of the increased thickness of laminated glass and the intrinsic low energy

absorption capability of the TPU interlayer, the normalized peak force and normalized absorbed energy of laminated glass actually reduced compared to plain sheet glass.

The appearance of the specimens after quasi-static penetration is presented in ***Figure 4(d)-(e)***. In contrast to the complete shattering of sheet glass, the BD HDPE/glass laminate still maintained some level of integrity even after full penetration, greatly improving the safety and security aspects for impact resistant glazing applications. Furthermore, the BD HDPE/glass laminate shows much greater out-of-plane deformation than sheet glass and laminated glass (see ***Figure 4(d)***). The normalized energy absorbed under low velocity penetration by the HDPE-reinforced laminate is more than 25 times higher than that of sheet glass or laminated glass, with 2.8 J/mm compared to 0.11 J/mm for sheet glass and 0.07 J/mm for laminated glass (see ***Figure 4(c)***). Delamination between HDPE layers is observed in the test region as well as in the surrounding areas (as shown in ***Figure 4(e)***). This extended delaminated area in BD HDPE/glass laminates contributes greatly to the higher overall energy absorption capability and greater penetration resistance. This increase in toughness can be attributed to the increased surfaces generated during delamination and tape pull-out, together with transverse splitting and fibrillation of the tapes. These fracture mechanisms together with crack deflection at the glass/TPU/HDPE interface may contribute to synergistic effects in energy absorption of the composites during penetration, which means that the work-of-fracture of the laminates can be higher than the cumulative fracture energies of the individual constituents[50].

It is also noteworthy that unlike the non-visible or barely-visible impact damage commonly observed in high performance composites like carbon fiber reinforced plastics (CFRP) and some glass fiber reinforced plastics (GFRP) under low-energy impact[51], the internal damage in the current HDPE/glass laminates can be observed by simple visual inspection, leading to a much

more efficient quality control and condition-based maintenance of the resulting composite component.

3.4 Optical properties of HDPE laminates with PC as outer layers

In the case of HDPE laminates with PC as the outer layers, the transmittance values at 550 nm are about 88 % for a single UD [0] HDPE/PC laminate, and about 83 % for 4-ply UD $[0]_4$ HDPE/PC laminate or BD $[0,90]_S$ HDPE/PC laminate, as shown in ***Figure 5(c)-(d)*** and Supporting Information ***Table S5***. The optical properties of these HDPE/PC laminates also follow the trend that transmittance values reduced by 1−2 % for every additional layer of TPU coated HDPE, regardless of its UD or BD structure. This additional drop in transmittance has the same physical origin as for laminates sandwiched between glass (see Section 3.2). Due to the larger refractive index difference between PC (n = 1.58−1.60)[40] and air ($n \approx 1$) compared to that of glass and air, a higher reflectance and light scattering and hence slightly lower transmittance can be expected. As a result, UD $[0]_4$ HDPE and BD $[0,90]_S$ HDPE laminates with PC as outer layers exhibit a slightly lower transparency (~ 2 % lower transmittance) as those sandwiched between glass (see ***Figure 5(a)-(b)***).

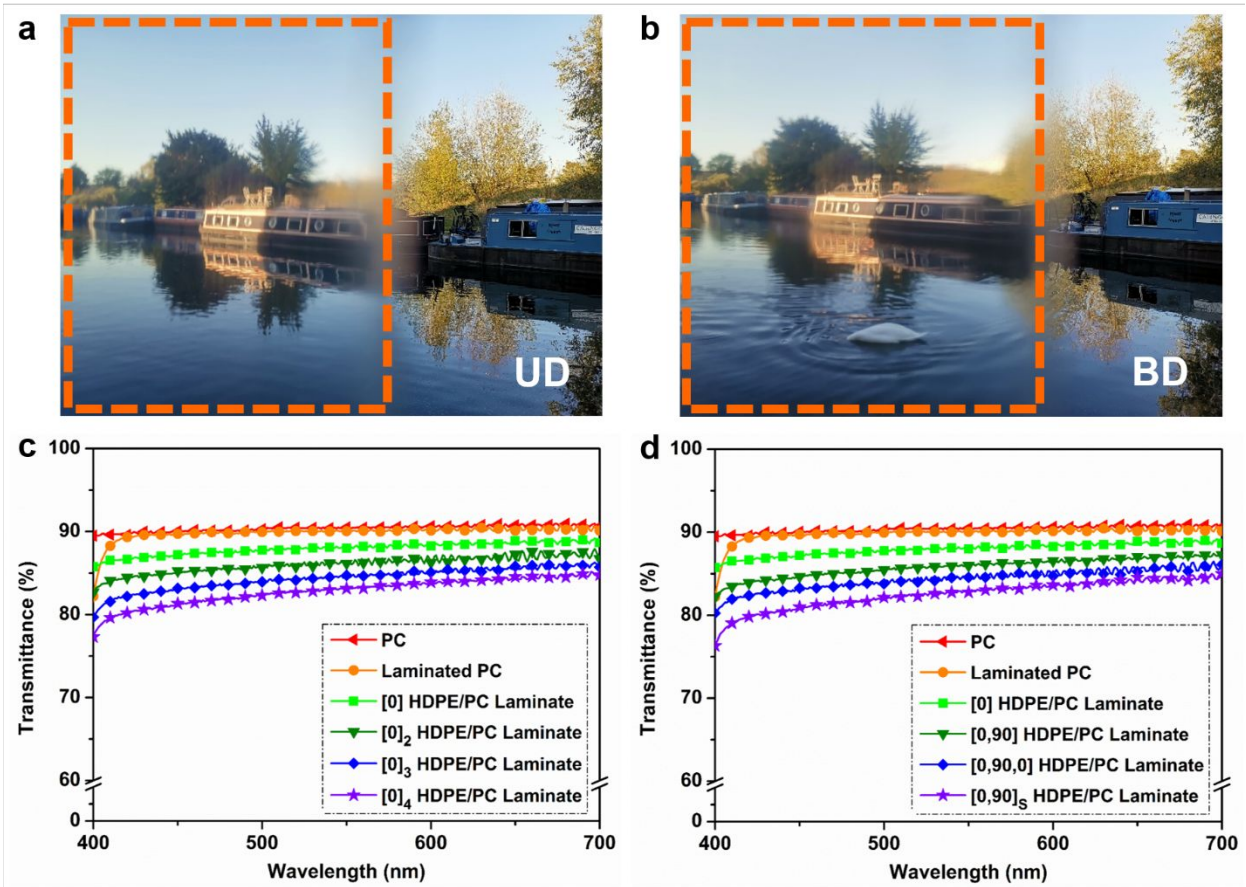

Figure 5. Optical appearance of (a) $[0]_4$ and (b) $[0,90]_S$ HDPE laminates with PC as outer layers when positioned in front of a distant scenery, revealing a transparent appearance for both UD and BD HDPE/PC laminates in the far field. For clarity, the dashed box sections in (a) and (b) mark the position of the laminates in front of the image. Transmittance spectra of (c) UD and (d) BD HDPE/PC laminates with different numbers (1, 2, 3, 4) of oriented HDPE layers measured at a sample-to-detector distance of 40 cm in the visible light range, showing a decrease in transmittance of about 1−2 % with every additional layer of TPU coated HDPE in the far field.

3.5 Tensile properties of HDPE laminates with PC as outer layers

Tensile tests on rectangular-shaped laminates with tapered end-taps as shown in ***Figure 6(a)*** were performed to obtain the Young's modulus, tensile strength, and strain at break for all specimens and the HDPE reinforcing efficiency was also evaluated by comparing experimental laminate data with theoretical data (see ***Table 3***) based on the generalized Rule of Mixtures (RoM) (eq. (5) and (6))[52]. In our case, oriented HDPE films are regarded as the reinforcing phase and PC together with TPU are considered as the matrix.

$$E_c = k\, E_{HDPE}V_{HDPE} + E_{PC}V_{PC} + E_{TPU}V_{TPU} \tag{5}$$

$$\sigma_c = k\, \sigma_{HDPE}V_{HDPE} + \sigma_{PC}V_{PC} + \sigma_{TPU}V_{TPU} \tag{6}$$

where E_c represents the Young's modulus of the composite laminate, σ_c represents the tensile strength of the composite. V_{HDPE}, V_{PC} and V_{TPU} are the volume fraction of the reinforcing HDPE phase, the PC and the TPU, respectively. $E_{HDPE,}$ E_{PC} and E_{TPU} are the Young's modulus of the HDPE film (12 GPa), the PC (2.9 GPa) and the TPU (0.15 GPa). σ_{HDPE} is the uniaxial tensile strength of the HDPE film (440 MPa) and σ_{PC} and σ_{TPU} are the stress in PC and TPU at the onset of HDPE failure (around 60 MPa for PC and 0.5 MPa for TPU). In the generalized RoM, k is the efficiency parameter. Based on our previous studies, uniaxially oriented polyethylene films typically have a transverse Young's modulus of about 2 GPa together with a transverse tensile strength of around 15 MPa, i.e. perpendicular to the machine direction[30], and hence these values are here used for theoretical calculations and prediction of composite properties.

Table 3. Tensile properties of UD $[0]_4$ HDPE and BD $[0,90]_S$ HDPE laminates with PC as outer layers.

Sample	Young's Modulus (GPa)	Theoretical Modulus (GPa)	Modulus Efficiency (%)	Tensile Strength (MPa)	Theoretical Strength (MPa)	Strength Efficiency (%)	Work-to-break × 10^6 (J/m^3)
Laminated PC	0.58 ± 0.09	0.66	87.8	12.5 ± 0.2	12.9	96.9	13.2 ± 3.1
UD HDPE/PC Laminate	4.64 ± 0.31	5.87	79.0	196 ± 17.0	205	95.4	124 ± 28.5
BD HDPE/PC Laminate	2.98 ± 0.14	3.68	81.0	113 ± 5.8	116	97.4	27.5 ± 8.4

It is shown in ***Table 3*** that UD $[0]_4$ HDPE laminates with PC as outer layers have a strength of 196 MPa and a modulus of 4.6 GPa, which is nearly 16 times and 8 times that of laminated PC with TPU as interlayers at a similar thickness, and 3.3 times and 1.6 times that of pure PC sheet (see Supporting Information ***Table S1***). The 4-ply UD HDPE/PC laminates display an almost 2 times higher work-to-break (i.e. the area below stress-strain curve) compared to PC sheet. The stress-strain curve of the UD HDPE/PC laminate as presented in ***Figure 6(b)*** shows an increasing stress up to an elongation (ε) of 23 %, followed by a gradual drop in stress without obvious yielding and necking until final fracture at $\varepsilon \sim 80$ %. Upon loading, the laminate delaminates first at the HDPE/TPU interface, followed by some transverse splitting of the oriented HDPE films. With further loading, the oriented HDPE films deform by yielding some plastic deformation, which is accompanied by whitening of the films before final fracture. The observed gradual drop in stress levels before final failure is attributed to the successive breakage of one or more HDPE films, as the laminate contains four layers of HDPE. As for the PC sheet and laminated PC, yielding occurs at $\varepsilon \sim 5$ % followed by some strain hardening until final fracture at $\varepsilon = 70-80$ %, with much less energy absorbed during the process compared to the UD HDPE-reinforced laminates.

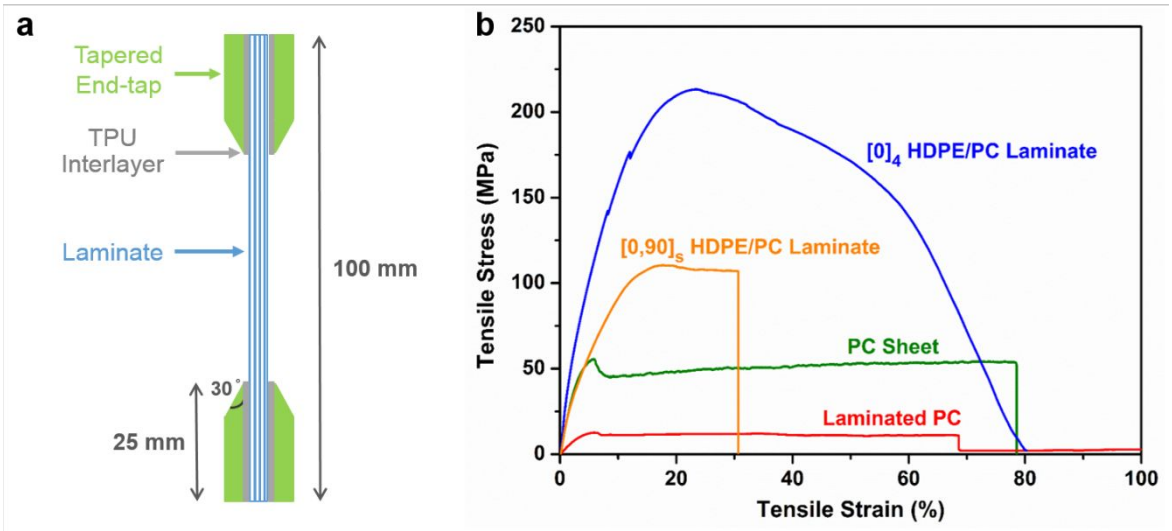

Figure 6. (a) Schematic illustration of the tensile test sample with tapered end-taps and (b) stress-strain curves of PC sheet, laminated PC, UD $[0]_4$ and BD $[0,90]_S$ HDPE laminates with PC as outer layers, showing a much improved work-to-break for laminates incorporating HDPE reinforcements as compared to pure PC sheet.

With regard to BD $[0,90]_S$ HDPE laminates with PC as outer layers, a nearly doubling in tensile strength value (113 MPa) together with a similar modulus value compared to pure PC sheet was found. As expected, UD HDPE/PC laminates exhibit a higher Young's modulus and tensile strength than BD HDPE/PC laminates as all four oriented PE films are effectively loaded along its principal materials' axis. BD laminate on the other hand have only half of the oriented films effectively loaded as a result of the cross-ply structure. Hence, the Young's modulus of the BD laminate is the weighted sum of the corresponding longitudinal and transverse moduli, with the transverse modulus of these oriented PE films being much lower than the longitudinal modulus (see Supporting Information ***Table S1***). The stress-strain curve of the BD HDPE/PC laminate showed a similar but lower trend to that for the UD laminate, except for a more sudden failure at a lower strain of around 30 %. This is mainly due to the relatively poor transverse mechanical

properties of the two uniaxially drawn HDPE films oriented at 90° direction, resulting in effectively only two reinforcing HDPE layers in the loading direction of the laminate. It is also noteworthy that the reinforcing efficiency *k* of the HDPE films is over 95 % for tensile strength, confirming the good stress transfer capability of the TPU interlayers and reinforcing effect of the oriented HDPE films in the laminates.

3.6 Penetration resistance of HDPE laminates with PC as outer layers

Figure 7(a) shows the contact force as a function of indenter displacement during the quasi-static penetration tests. PC sheet and laminated PC were directly penetrated at an indenter displacement of about 13 mm, with the load dropping instantaneously to nearly zero after the peak force was reached, indicating brittle fracture. A much lower contact force was measured for laminated PC compared to pure PC sheet due to presence of the soft TPU interlayers. With the addition of four plies of HDPE, the BD $[0,90]_S$ HDPE laminate with PC as outer layers reached a slightly higher maximum peak force of 1859 N/mm at a similar indentation of around 11 mm, followed by successive drops before final penetration at an indentation of around 18.5 mm. Clearly, the BD HDPE/PC laminate was still able to withstand continued loading and deformation even after reaching the peak force, indicative of a greater damage tolerance with a gradual load drop rather than a sudden load drop and catastrophic failure. As shown in ***Figure 7(b)-(c)***, BD HDPE/PC laminates can absorb nearly 6 times the energy required for penetration and show a 8 times higher peak force in comparison to laminated PC without the HDPE reinforcement. It also shows an equally high penetration energy and peak force as pure PC sheet.

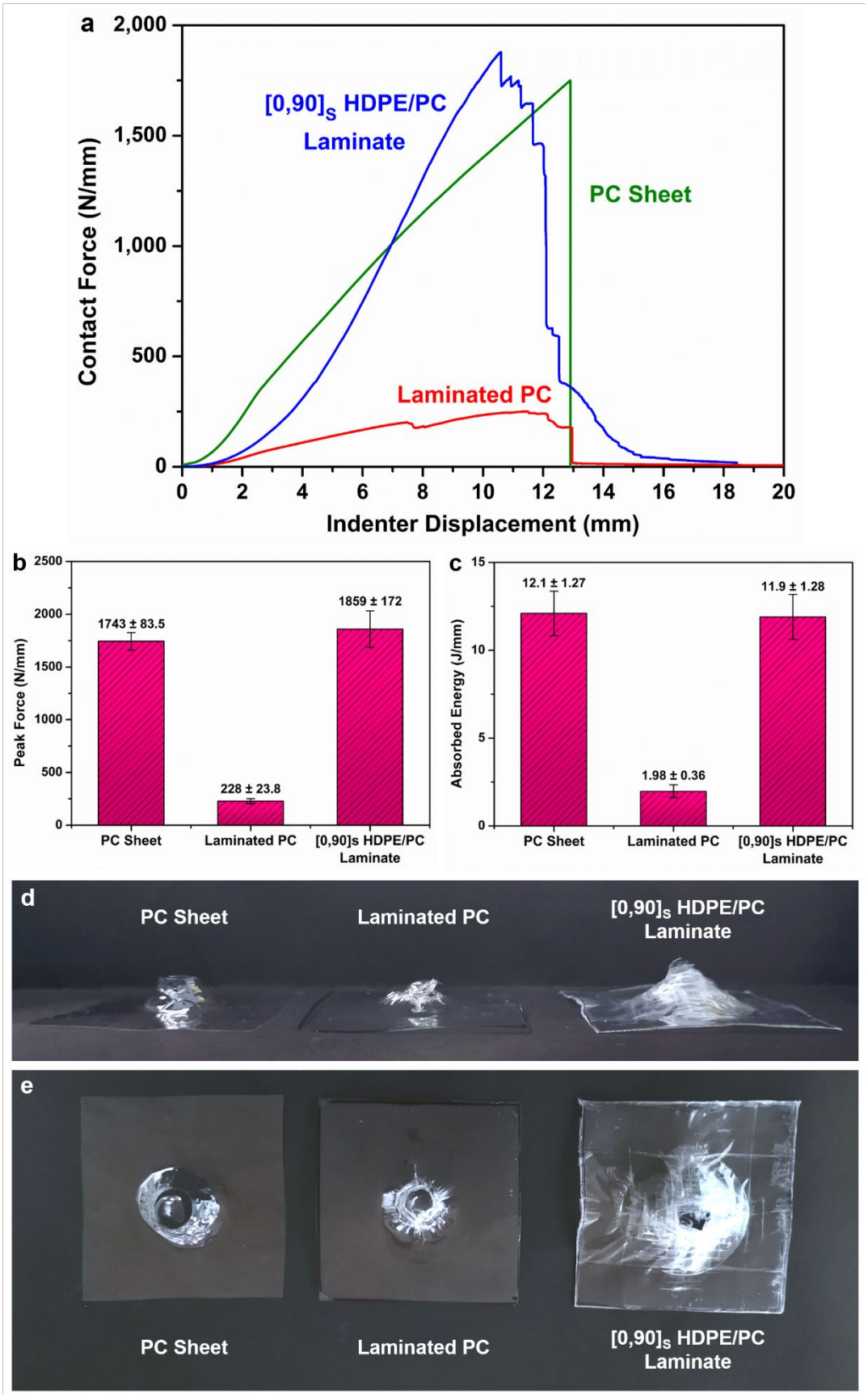
a
Contact Force (N/mm)
Indenter Displacement (mm)
[0,90]S HDPE/PC Laminate
PC Sheet
Laminated PC
b
Peak Force (N/mm)
1743 ± 83.5
228 ± 23.8
1859 ± 172
PC Sheet
Laminated PC
[0,90]s HDPE/PC Laminate
c
Absorbed Energy (J/mm)
12.1 ± 1.27
1.98 ± 0.36
11.9 ± 1.28
PC Sheet
Laminated PC
[0,90]s HDPE/PC Laminate
d
PC Sheet
Laminated PC
[0,90]S HDPE/PC Laminate
e
PC Sheet
Laminated PC
[0,90]S HDPE/PC Laminate

Figure 7. The penetration resistance of BD HDPE transparent composites with PC as outer layers: (a) contact force versus indenter displacement, (b) absorbed energy and (c) peak force of PC sheet, laminated PC and BD $[0,90]_S$ HDPE/PC laminate, showing that the BD HDPE/PC laminate displays a similar performance to PC but with a much higher energy absorption and peak force compared to laminated PC. (d) Edge-side view of specimens with clear out-of-plane deformation and (e) bottom-side view after full penetration of PC sheet, laminated PC and BD $[0,90]_S$ HDPE laminate sandwiched between PC, showing the largest area of deformation for the BD HDPE/PC laminate. Contact force, absorbed energy and peak force are all normalized by specimen thickness.

Images of fully penetrated specimens are shown in ***Figure 7(d)-(e)***. They show a relatively small and localized out-of-plane deformation area with mainly yielding and plastic deformation. On the other hand, the BD $[0,90]_S$ HDPE/PC laminate consisting of four layers of oriented high performance HDPE films experienced many different stages of deformation upon loading before ultimate penetration. Failure modes range from delamination between HDPE layers, to tape fibrillation and lateral fracture of HDPE tapes. These fracture processes all contribute to the high level of energy absorption during penetration, as well as the large deformed area and out-of-plane deformation.

A few critical remarks are appropriate with respect to the results presented here. Most importantly, UD $[0]_4$ HDPE/glass laminates, as expected, exhibit birefringence between crossed polarizers (see Supporting Information ***Figure S4(a)***). Under specific illumination conditions (e.g. low incoming angle of direct sunlight), this birefringence can cause undesired optical effects such as the appearance of colors originating from polarization and wavelength dispersion effects[53]. Usually, these effects can be reduced efficiently by designing 0/90 cross-ply BD laminates and by compensation of the optical retardation ($d\Delta n$) in two or three dimensions. In the Supporting

Information (***Figure S4(b)***), it is shown that optical compensation is only partly achieved in BD $[0,90]_S$ HDPE/glass laminates which is probably related to thickness fluctuations in our stretched HDPE films and impurities like dust trapped within the laminates. It is anticipated that these technical issues can be resolved in an optimized manufacturing environment.

Although the PC outer layers exhibit a more ductile failure mode compared to laminates sandwiched between glass, the susceptibility to ultraviolet (UV) exposure and relatively low scratch resistant nature of PC may result in reduced levels of optical transmittance after long-term usage. On the other hand, the HDPE laminates with glass as outer layers may maintain their clear appearance after prolonged use especially if proper stabilizers are used in the HDPE. However, the nature of glass can lead to brittle fracture and cracking of the sheet glass in the laminates, whereas PC is more flexible and fails by yielding. Therefore, depending on the requirements of the application, the most appropriate outer layer for these laminates should be selected. The number of reinforcing HDPE layers can also be adjusted according to the balance required between optical and mechanical properties, since an increase in number of HDPE layers for greater mechanical performance may lead to a sacrifice in optical clarity.

The manufactured highly transparent, lightweight composite laminates with good mechanical performance outperformed many existing transparent materials, showing great potential to replace conventional inorganic glass or polymeric transparent materials including PMMA and PC and to become a new generation of laminated materials that combine high clarity and high mechanical performance. With this new class of transparent laminated composites, many potential applications can be envisaged, including structural glazing elements, automotive and aerospace glazing, windshields, protective visors, and displays for electronic devices.

4. Conclusions

High performance transparent composite laminates based on highly oriented HDPE films sandwiched between either glass or PC have been successfully manufactured with a good combination of high optical transparency, good tensile properties and penetration resistance. TPU was selected as the interlayer material of choice because of its higher refractive index and better wetting and bonding properties compared to other evaluated adhesives. Far field transmittance values of around 85−90 % at 550 nm were achieved in laminates consisting of 1−4 layers of HDPE films with glass as outer layers, while about 2 % lower transmittance values were reported for corresponding specimens sandwiched between PC. It was also found that transmittance dropped by 1−2 % with every additional layer of TPU coated HDPE due to increased reflections and light scattering at interfaces, regardless of a UD or BD lay-up within the laminates.

In terms of mechanical performance, good penetration resistance was achieved in BD $[0,90]_S$ HDPE laminates with glass as outer layers. Such laminates were able to absorb more than 25 times the energy required for full penetration compared to sheet glass or laminated glass. The high mechanical performance of these laminates was mainly attributed to the high strength and stiffness of the oriented HDPE films, together with good load transfer between layers by TPU interlayers. Apart from a high reinforcing efficiency of the HDPE films in terms of both modulus and strength, UD $[0]_4$ HDPE laminate with PC as outer layers also demonstrated a two times higher tensile strength and work-to-break compared to that of pure PC.

Due to the excellent combination of high tensile strength, penetration resistance and far field optical transparency, the fabricated HDPE laminates with either glass or PC as outer layers show great potential for replacing traditional inorganic glass or polymeric glasses like PC and PMMA

for applications in structural glazing for buildings, automotive and aerospace, windshields, visors, displays, etc.

Conflict of interest

The authors declare no competing interests.

Acknowledgements

We gratefully thank Sichuan Longhua Film Co., Ltd for offering the PC sheets and Schweitzer-Mauduit International, Inc. (USA) for providing TPU films. Y. Lin greatly acknowledges financial support by the China Scholarship Council (CSC).

Associated Content

Supporting Information

The Supporting Information is available free of charge at DOI.

Mechanical properties of laminate constituent materials (Table S1); transmittance spectra of interlayer materials (Figure S1); DSC curves of laminate constituent materials (Figure S2); stress-strain curves of interlayer materials (Figure S3); mechanical properties of interlayer materials (Table S2); contact angles and surface free energies of laminate constituent materials (Table S3); transmittance values of UD and BD laminates sandwiched between glass (Table S4); transmittance

values of UD and BD laminates sandwiched between PC (Table S5); optical images of UD and BD laminates under crossed polarizers. (PDF)

References

1. Peijs, T.; Venderbosch, R. W.; Lemstra, P. J. Hybrid composites based on polyethylene and carbon fibres Part 3: Impact resistant structural composites through damage management. *Composites* **1990,** *21* (6), 522-530.
2. Lowe, J. 11 - Aerospace applications. In *Design and Manufacture of Textile Composites*; Long, A. C., Ed.; Woodhead Publishing: 2005; pp 405-423.
3. Zhang, H.; Bilotti, E.; Peijs, T. Nano-Engineered Hierarchical Carbon Fibres and Their Composites: Preparation, Properties and Multifunctionalities. In *The Structural Integrity of Carbon Fiber Composites: Fifty Years of Progress and Achievement of the Science, Development, and Applications*; Beaumont, P. W. R.; Soutis, C.; Hodzic, A., Eds.; Springer International Publishing: Cham, 2017; pp 101-116.
4. Li, H.; Richards, C.; Watson, J. High-Performance Glass Fiber Development for Composite Applications. *International Journal of Applied Glass Science* **2014,** *5* (1), 65-81.
5. Peijs, T. 6.7 Electrospun Polymer Nanofibers and Their Composites. In *Comprehensive Composite Materials II*; Beaumont, P. W. R.; Zweben, C. H., Eds.; Elsevier: Oxford, 2018; pp 162-200.

6. Peijs, T. 1.5 High performance polyethylene fibers. In *Comprehensive Composite Materials II*; Beaumont, P. W. R.; Zweben, C. H., Eds.; Elsevier: Oxford, 2018; Chapter 1.5, pp 86-126.

7. Tabiei, A.; Nilakantan, G. Ballistic Impact of Dry Woven Fabric Composites: A Review. *Appl. Mech. Rev.* **2008,** *61* (1), 010801.

8. Zhang, T. G.; Satapathy, S. S.; Vargas-Gonzalez, L. R.; Walsh, S. M. Ballistic impact response of Ultra-High-Molecular-Weight Polyethylene (UHMWPE). *Compos. Struct.* **2015,** *133*, 191-201.

9. Wang, Q.; Chen, Z.; Chen, Z. Design and characteristics of hybrid composite armor subjected to projectile impact. *Mater. Des.* **2013,** *46*, 634-639.

10. Tham, C. Y.; Tan, V. B. C.; Lee, H. P. Ballistic impact of a KEVLAR® helmet: Experiment and simulations. *Int. J. Impact Eng.* **2008,** *35* (5), 304-318.

11. Krug Iii, D. J.; Asuncion, M. Z.; Popova, V.; Laine, R. M. Transparent fiber glass reinforced composites. *Compos. Sci. Technol.* **2013,** *77*, 95-100.

12. Menta, V. G. K.; Vuppalapati, R. R.; Chandrashekhara, K.; Schuman, T. Manufacturing of Transparent Composites Using Vacuum Infusion Process. *Polym. Polym. Compos.* **2014,** *22* (9), 843-850.

13. Velez, M.; Schuman, T.; Day, D. Optical properties of optically transparent glass-ribbon composites. *J. Compos. Mater.* **2014,** *48* (30), 3747-3754.

14. Velez, M.; Braisted, W.; Frank, G.; Phillips, P.; Day, D.; McLaughlin, M. Impact strength of optically transparent glass ribbon composites. *J. Compos. Mater.* **2012,** *46* (14), 1677-1695.

15. Bergshoef, M. M.; Vancso, G. J. Transparent Nanocomposites with Ultrathin, Electrospun Nylon-4,6 Fiber Reinforcement. *Adv. Mater.* **1999,** *11* (16), 1362-1365.

16. Krauthauser, C.; Deitzel, J. M.; O'Brien, D.; Hrycushko, J. Optical Properties of Transparent Resins with Electrospun Polymer Nanofibers. In *Polymeric Nanofibers*; American Chemical Society: 2006; Chapter 25, pp 353-369.

17. Yano, H.; Sugiyama, J.; Nakagaito, A. N.; Nogi, M.; Matsuura, T.; Hikita, M.; Handa, K. Optically Transparent Composites Reinforced with Networks of Bacterial Nanofibers. *Adv. Mater.* **2005,** *17* (2), 153-155.

18. Liao, H.; Wu, Y.; Wu, M.; Zhan, X.; Liu, H. Aligned electrospun cellulose fibers reinforced epoxy resin composite films with high visible light transmittance. *Cellulose* **2012,** *19* (1), 111-119.

19. Pinto, E. R. P.; Barud, H. S.; Silva, R. R.; Palmieri, M.; Polito, W. L.; Calil, V. L.; Cremona, M.; Ribeiro, S. J. L.; Messaddeq, Y. Transparent composites prepared from bacterial cellulose and castor oil based polyurethane as substrates for flexible OLEDs. *J. Mater. Chem. C* **2015,** *3* (44), 11581-11588.

20. O'Brien, D. J.; Parquette, B.; Hoey, M. L.; Perry, J. The design and performance of a polymer ribbon-reinforced transparent composite material. *Polym. Compos.* **2018,** *39* (7), 2523-2534.

21. Haldimann, M.; Luible, A.; Overend, M. *Structural use of glass*, Labse: 2008; Vol. 10.

22. Vedrtnam, A.; Pawar, S. J. Laminated plate theories and fracture of laminated glass plate – A review. *Eng. Fract. Mech.* **2017,** *186*, 316-330.

23. Abid, H. M.; Shah, Q. H.; Ibrahim, M. S. Perforation of Polycarbonate Sheet When Subjected to Impact Test–A Review. *International Journal of Applied Engineering Research* **2017,** *12* (24), 14514-14522.

24. Rühl, A.; Kolling, S.; Schneider, J. Characterization and modeling of poly(methyl methacrylate) and thermoplastic polyurethane for the application in laminated setups. *Mech. Mater.* **2017,** *113*, 102-111.

25. Martín, M.; Centelles, X.; Solé, A.; Barreneche, C.; Fernández, A. I.; Cabeza, L. F. Polymeric interlayer materials for laminated glass: A review. *Construction and Building Materials* **2020,** *230*, 116897.

26. Harper, C. A.; Petrie, E. M. *Plastics materials and processes: a concise encyclopedia*, John Wiley & Sons: 2003.

27. Lin, Y.; Patel, R.; Cao, J.; Tu, W.; Zhang, H.; Bilotti, E.; Bastiaansen, C. W. M.; Peijs, T. Glass-like transparent high strength polyethylene films by tuning drawing temperature. *Polymer* **2019,** *171*, 180-191.

28. Lin, Y.; Tu, W.; Verpaalen, R. C. P.; Zhang, H.; Bastiaansen, C. W. M.; Peijs, T. Transparent, Lightweight, and High Strength Polyethylene Films by a Scalable Continuous Extrusion and Solid-State Drawing Process. *Macromol. Mater. Eng.* **2019,** *304* (8), 1900138.

29. Lin, Y.; Peijs, T.; Bastiaansen, C. W. M. Transparent Drawn Article. GB1820429.7, 2018.

30. Peijs, T.; Rijsdijk, H. A.; de Kok, J. M. M.; Lemstra, P. J. The role of interface and fibre anisotropy in controlling the performance of polyethylene-fibre-reinforced composites. *Compos. Sci. Technol.* **1994,** *52* (3), 449-466.

31. Campbell, F. C. *Structural composite materials*, ASM international: 2010.

32. Alcock, B.; Peijs, T. Technology and Development of Self-Reinforced Polymer Composites. In *Polymer Composites – Polyolefin Fractionation – Polymeric Peptidomimetics – Collagens*; Abe, A.; Kausch, H.-H.; Möller, M.; Pasch, H., Eds.; Springer Berlin Heidelberg: Berlin, Heidelberg, 2013; pp 1-76.

33. Owens, D. K.; Wendt, R. C. Estimation of the surface free energy of polymers. *J. Appl. Polym. Sci.* **1969,** *13* (8), 1741-1747.

34. Good, R. J.; Girifalco, L. A theory for estimation of surface and interfacial energies. III. Estimation of surface energies of solids from contact angle data. *The Journal of Physical Chemistry* **1960,** *64* (5), 561-565.

35. Good, R. J. Contact angle, wetting, and adhesion: a critical review. *J. Adhes. Sci. Technol.* **1992,** *6* (12), 1269-1302.

36. Liu, Y.; Zhang, H.; Porwal, H.; Tu, W.; Wan, K.; Evans, J.; Newton, M.; Busfield, J. J. C.; Peijs, T.; Bilotti, E. Tailored pyroresistive performance and flexibility by introducing a secondary thermoplastic elastomeric phase into graphene nanoplatelet (GNP) filled polymer composites for self-regulating heating devices. *J. Mater. Chem. C* **2018,** *6* (11), 2760-2768.

37. ASTM D1876-08(2015)e1, Standard Test Method for Peel Resistance of Adhesives (T-Peel Test), ASTM International, West Conshohocken, PA, 2015, www.astm.org.

38. ASTM D3039 / D3039M-17, Standard Test Method for Tensile Properties of Polymer Matrix Composite Materials, ASTM International, West Conshohocken, PA, 2017, www.astm.org.

39. ASTM D6264 / D6264M-17, Standard Test Method for Measuring the Damage Resistance of a Fiber-Reinforced Polymer-Matrix Composite to a Concentrated Quasi-Static Indentation Force, ASTM International, West Conshohocken, PA, 2017, www.astm.org.

40. Waxler, R. M.; Horowitz, D.; Feldman, A. Optical and physical parameters of Plexiglas 55 and Lexan. *Appl. Opt.* **1979,** *18* (1), 101-104.

41. Vasile, C.; Pascu, M. *Practical guide to polyethylene*, iSmithers Rapra Publishing: 2005.

42. Bistac, S.; Kunemann, P.; Schultz, J. Crystalline modifications of ethylene-vinyl acetate copolymers induced by a tensile drawing: effect of the molecular weight. *Polymer* **1998,** *39* (20), 4875-4881.

43. Dhaliwal, A. K.; Hay, J. N. The characterization of polyvinyl butyral by thermal analysis. *Thermochim. Acta* **2002,** *391* (1), 245-255.

44. Wang, D.; Zhang, Z.; Li, Y.; Xu, C. Highly Transparent and Durable Superhydrophobic Hybrid Nanoporous Coatings Fabricated from Polysiloxane. *ACS Appl. Mater. Interfaces* **2014,** *6* (13), 10014-10021.

45. Wang, Z.; Lu, Z.; Mahoney, C.; Yan, J.; Ferebee, R.; Luo, D.; Matyjaszewski, K.; Bockstaller, M. R. Transparent and High Refractive Index Thermoplastic Polymer Glasses Using Evaporative Ligand Exchange of Hybrid Particle Fillers. *ACS Appl. Mater. Interfaces* **2017,** *9* (8), 7515-7522.

46. ASTM D1746-15, Standard Test Method for Transparency of Plastic Sheeting, ASTM International, West Conshohocken, PA, 2015, www.astm.org.

47. Ajji, A.; Zhang, X.; Elkoun, S. Biaxial orientation in HDPE films: comparison of infrared spectroscopy, X-ray pole figures and birefringence techniques. *Polymer* **2005,** *46* (11), 3838-3846.

48. Chatterjee, T.; Patel, R.; Garnett, J.; Paradkar, R.; Ge, S.; Liu, L.; Forziati, K. T.; Shah, N. Machine direction orientation of high density polyethylene (HDPE): Barrier and optical properties. *Polymer* **2014,** *55* (16), 4102-4115.

49. Mai, F.; Tu, W.; Bilotti, E.; Peijs, T. Preparation and properties of self-reinforced poly(lactic acid) composites based on oriented tapes. *Compos. Part A - Appl. S.* **2015,** *76*, 145-153.

50. Peijs, T.; Smets, E. A. M.; Govaert, L. E. Strain rate and temperature effects on energy absorption of polyethylene fibres and composites. *Appl. Compos. Mater.* **1994,** *1* (1), 35-54.

51. Davies, G. A. O.; Zhang, X. Impact damage prediction in carbon composite structures. *Int. J. Impact Eng.* **1995,** *16* (1), 149-170.

52. Clyne, T.; Hull, D. *An introduction to composite materials*, Cambridge university press: 2019.

53. Shimada, H.; Nobukawa, S.; Hattori, T.; Yamaguchi, M. Wavelength dispersion of birefringence of oriented polyethylene films. *Appl. Opt.* **2017,** *56* (13), 3806-3811.